AD-A086 799   DAYTON UNIV OH RESEARCH INST   F/G 20/4
SIMULATION OF VISCOUS STEADY FLOW PAST AN ARBITRARY TWO-DIMENSI--ETC(U)
FEB 80 M NAPOLITANO   F33615-76-C-3145
UNCLASSIFIED   AFWAL-TR-80-3038   NL

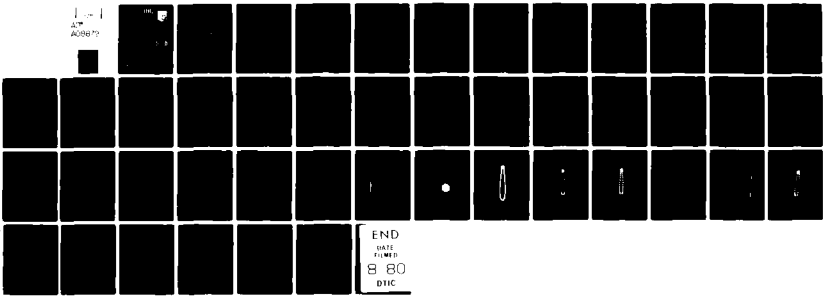

AFWAL-TR-80-3038 LEVEL II

2

ADA086799

SIMULATION OF VISCOUS STEADY FLOW PAST AN ARBITRARY TWO-DIMENSIONAL BODY

MICHELE NAPOLITANO
UNIVERSITY OF DAYTON RESEARCH INSTITUTE
300 COLLEGE PARK
DAYTON, OHIO 45469

FEBRUARY 1980

TECHNICAL REPORT AFWAL-TR-80-3038
Final Report for period August 1979 — January 1980

FLIGHT DYNAMICS LABORATORY
AIR FORCE WRIGHT AERONAUTICAL LABORATORIES
AIR FORCE SYSTEMS COMMAND
WRIGHT-PATTERSON AIR FORCE BASE, OHIO 45433

NOTICE

When Government drawings, specifications, or other data are used for any purpose other than in connection with a definitely related Government procurement operation, the United States Government thereby incurs no responsibility nor any obligation whatsoever; and the fact that the government may have formulated, furnished, or in any way supplied the said drawings, specifications, or other data, is not to be regarded by implication or otherwise as in any manner licensing the holder or any other person or corporation, or conveying any rights or permission to manufacture, use, or sell any patented invention that may in any way be related thereto.

This report has been reviewed by the Information Office (PA) and is releasable to the National Technical Information Service (NTIS). At NTIS, it will be available to the general public, including foreign nations.

This technical report has been reviewed and is approved for publication.

William L Hankey

PROJECT ENGINEER

Lowell C Keel

LOWELL C. KEEL, Maj, USAF
Chief, Aerodynamics & Airframe Branch

FOR THE COMMANDER

Peter J Butkewicz

PETER J. BUTKEWICZ, Colonel, USAF
Chief, Aeromechanics Division

"If your address has changed, if you wish to be removed from our mailing list, or if the addressee is no longer employed by your organization please notify AFWAL/FIMM *,W-PAFB, OH 45433 to help us maintain a current mailing list".*

Copies of this report should not be returned unless return is required by security considerations, contractual obligations, or notice on a specific document.

SECURITY CLASSIFICATION OF THIS PAGE (When Data Entered)

REPORT DOCUMENTATION PAGE

READ INSTRUCTIONS BEFORE COMPLETING FORM

1. REPORT NUMBER: AFWAL-TR-80-3038	2. GOVT ACCESSION NO.: AD-A086 799
3. RECIPIENT'S CATALOG NUMBER	
4. TITLE (and Subtitle): Simulation of Viscous Steady Flow Past An Arbitrary Two-Dimensional Body.	5. TYPE OF REPORT & PERIOD COVERED: FINAL REP[redacted]. August [redacted]79 — Jan[redacted] [redacted]80
	6. PERFORMING ORG. REPORT NUMBER
7. AUTHOR(s): Dr. Michele Napolitano	8. CONTRACT OR GRANT NUMBER(s): F33615-76-C-3145
9. PERFORMING ORGANIZATION NAME AND ADDRESS: University of Dayton Research Institute, 300 College Park, Dayton, Ohio 45469	10. PROGRAM ELEMENT, PROJECT, TASK AREA & WORK UNIT NUMBERS: Project 2307N436 — IN4
11. CONTROLLING OFFICE NAME AND ADDRESS: Air Force Wright Aeronautical Labs (AFSC), Wright-Patterson AFB, Ohio 45433	12. REPORT DATE: Feb[redacted] [redacted]80
	13. NUMBER OF PAGES
14. MONITORING AGENCY NAME & ADDRESS (if different from Controlling Office): 46	15. SECURITY CLASS. (of this report): Unclassified
	15a. DECLASSIFICATION/DOWNGRADING SCHEDULE

16. DISTRIBUTION STATEMENT (of this Report)

Approved for public release; distribution unlimited

17. DISTRIBUTION STATEMENT (of the abstract entered in Block 20, if different from Report)

18. SUPPLEMENTARY NOTES

19. KEY WORDS (Continue on reverse side if necessary and identify by block number)

Numerical Solution

Incompressible, Laminar Viscous Flow

Alternating Direction Implicit (ADI) Technique

Body-Oriented Coordinates

20. ABSTRACT (Continue on reverse side if necessary and identify by block number)

A numerical technique is developed for solving laminar steady flow past an arbitrary two-dimensional body. A system of body oriented coordinates is first generated numerically by means of the transformation of Thompson et al. The vorticity-stream function Navier-Stokes equations are then solved by the Alternating Direction Implicit procedure of Douglas and Gunn. A relaxation-like time derivative is added to the stream function equation and the vorticity equation is linearized in time so that only the converged steady solution has

DD FORM 1473, 1 JAN 73 — EDITION OF 1 NOV 65 IS OBSOLETE

SECURITY CLASSIFICATION OF THIS PAGE (When Data Entered)

105400

physical meaning. Numerical results are presented for two model problems (a one dimensional Poiseuille flow and the driven cavity problem) and for flow past a NACA 0012 airfoil for moderate to high values of the Reynolds Number. Finally, advantages and limitations for the proposed algorithm are briefly addressed.

FOREWORD

This report is the result of the work performed by Dr. Michele Napolitano, visiting scientist in the AFWAL/FIMM, from August 1979 to January 1980, under Project Number 2307N436, "Computational Fluid Dynamics," whose AFWAL Task Engineer, was Dr. Wilbur L. Hankey.

The author is very grateful to Dr. Hankey for his interest and encouragement to all the members of the Computational Aerodynamics Group for the very pleasant and cooperative environment they have provided. Captain H. A. Hegna is acknowledged for providing the coordinate transformation used in this work and Professor R. T. Davis for his helpful suggestions and comments.

TABLE OF CONTENTS

LIST OF FIGURES

LIST OF SYMBOLS

a1,b1,c1,d1,e1,f1,h1, a2,b2,c2,d2,e2,f2,h2	Coefficients of the two coupled tridiagonal equations
J	Jacobian of the coordiante transformation
h	Height of the channel for the Poiseuille flow
Re	Reynolds number
R1,S1,T1,R2,S2,T2	Recursion coefficients for the solution of the two coupled tridiagonal equations
t	(nondimensional) Time
x	(nondimensional) Horizontal coordinate
y	(nondimensional) Vertical coordinate

Greek Symbols

$\alpha,\beta,\gamma,\sigma,\tau$	Scale factors of the coordinate transformation
Δ	Step size
∂	Partial derivative sign
η	Transformed vertical coordinate
θ	Angle of attack
ξ	Transformed horizontal coordinate
ψ	Stream function
ω	Vorticity
$\bar{\psi}$	Incremental stream function
$\bar{\omega}$	Incremental vorticity

subscripts

$1,..,i-1,i,i+1,..,I$	Longitudinal grid points
$1,..,j-1,j,j+1,..,J$	Vertical grid points
c	Belonging to the circle having the center in the origin and radius equal to one
M	Maximum
t,x,y,η,ξ	Partial derivative with respect to the indicated variable

superscripts

$n,*,n+1$	Initial, intermediate and final levels of the ADI numerical technique

SECTION I

INTRODUCTION

In the last two decades there has been remarkable technical progress in the fields of electronics, in general, and data processing, in particular. In the same period, the new area of computational fluid dynamics, a branch of numerical analysis, has experienced a growth comparable to that of computer technology. Among the many applications of computational fluid dynamics, the numerical solution of the Navier-Stokes equations has challenged a large number of engineers and scientists, due to the capability of these partial differential equations of correctly modeling most of the very interesting phenomena associated with fluid viscosity and compressibility (e.g. shocks, shock-boundary-layer interaction, separation, stall, etc.).

The present work is concerned with the problem of low speed viscous flow past an arbitrary two-dimensional body, for which all compressibility effects are negligible. Even for the case of the incompressible Navier-Stokes equations, the number of numerical techniques and their applications, available in the technical literature, is so high that no systematic survey will be provided here. For the present purpose, only a few typical examples will be mentioned: the pioneering work of Burggraf[1] concerning the now classical driven cavity problem; the studies of Davis and his co-workers[2-4] for laminar flow past several semi-infinite bodies at moderate to high values of the Reynolds number; the analysis of Mehta and Lavan[5] about the starting vortex, separation and stall of a lifting airfoil. However, most numerical techniques[2-5] are limited to particular geometries, for which a coordinate transformation, mapping the body surface into a coordinate line, or equivalently the potential flow solution could be obtained

analytically. Two approaches appear at present very promising for removing such a difficulty and providing viscous flow solutions about arbitrary configurations: The Finite Element Method and the numerical generation of body oriented coordinates. In particular, Thompson et al[6-10] have developed and improved, throughout the years, a numerical technique for solving the time dependent Navier-Stokes equations past one or more arbitrary two dimensional bodies: First, they generate an appropriate body-fitted coordinate system which maps the flow domain of arbitrary shape in the physical plane into a rectangle in the transformed plane. Second, they solve the unsteady Navier-Stokes equations in the transformed plane (coordinates) by means of an implicit time marching numerical technique. A point SOR (Successive Over Relaxation) iterative procedure is used at each new time level in order to solve for the nonlinear terms and the elliptic part of the equations, explicitly. This approach has been shown to be applicable to both the vorticity-stream function[8] and pressure velocity[9,10] formulations of the time-dependent Navier-Stokes equations, for laminar as well as turbulent flows. Further, it has been proved very reliable in modeling highly separated flows around stalled airfoils[10]. However, its use for design purposes is severely limited by its computational inefficiency. In particular, when it is used to provide a steady-state flow solution by following the asymptotic time decay of an unsteady flow phenomenon, the intrinsic inefficiency of point iterative methods compounds to that of time dependent approaches.

The aim of the present research is to develop an efficient numerical procedure for solving the steady-state Navier-Stokes equations past an arbitrary two dimensional body, by combining the transformation of Thompson et al[6,7] with a numerical technique more efficient than the point SOR method.

Recently, many researchers have applied a number of ADI (Alternating Direction Implicit) techniques to the numerical solution of the Navier-Stokes Equations. In particular, Davis and his co-workers[2-4,15], Briley and McDonald[11-13] and Beam and Warming[14] have obtained considerable success with such a technique. The two major advantages of the Linearized Block Implicit methods[13] (like the ADI) are the (quasi)linearization of the governing equations, which eliminates any need of iterations at any time level, and the presence of only block-tridiagonal matrices, whose direct inversion is performed very efficiently by block Gaussian elimination[16]. In the present study an ADI technique will be used to solve the vorticity-stream function Navier-Stokes equations in the transformed plane after mapping the flow field around an arbitrary airfoil into a rectangle by means of the transformation of Thompson et al[6,7]. Since only the steady state solution is of present concern, the stream function equation is parabolized by adding to it a relaxation-like time derivative, according to Davis[2]. The vorticity equation is then (quasi)linearized and the two (equations) are solved as a coupled set of finite difference equations by means of the Douglas and Gunn[17] ADI technique. The incremental approach of Briley and McDonald[12] also used by Beam and Warming[14] and by Davis and Hill[15] is used at the second sweep of the ADI procedure, in order to minimize computer storage.

The coordinate transformation[6,7], employed here, introduces a cut in the physical plane, which is mapped into the two vertical sides of the integration rectangle in the transformed plane. Therefore, the additional difficulty of periodic boundary conditions in the horizontal direction had to be dealt with. To this end, the method of Ahlberg et al.[18] for inverting a tridiagonal periodic matrix has been generalized to the present case of

a two-by-two periodic block tridiagonal matrix. All the details of the algorithm and the results of its application to a simple model problem are given in the Appendix.

The present numerical technique has been applied to three problems. First, a simple Poiseuille flow has been computed in order to verify the second order accuracy of the method versus an exact analytical solution. Second, the classical driven cavity problem[1] has also been solved to further verify the proposed algorithm in the case of a truly two-dimensional flow problem. Finally, the flow past a NACA 0012 airfoil has been computed to demonstrate the capability of simulating the viscous steady flow past an arbitrary two-dimensional body.

SECTION II

GOVERNING EQUATIONS AND COORDINATE TRANSFORMATION

The governing equations are the nondimensional vorticity stream function Navier-Stokes Equations, with a relaxation-like time derivative, $\frac{\partial \psi}{\partial t}$, added to the stream function equation[2] in order to parabolize it:

$$\frac{\partial \omega}{\partial t} + \psi_y \omega_x - \psi_x \omega_y = 1/Re(\omega_{xx} + \omega_{yy}) \tag{1}$$

and

$$\psi_{xx} + \psi_{yy} + \omega = \frac{\partial \psi}{\partial t} \tag{2}$$

Equations (1) and (2) constitute a set of parabolic (in time) partial differential equations which can be solved numerically by means of a time marching ADI procedure. However, it is important to realize that, since equations (1) and (2) are not the unsteady Navier-Stokes equations, a correct description of the transient is not provided and only the converged solution will have physical meaning.

In order to solve equations (1) and (2) for flow past an arbitrary two-dimensional body (e.g. an airfoil), the transformation of Thompson et al.[6,7] is used to generate numerically a system of body oriented coordinates. With this transformation[6,7] the flow field in the physical plane, comprised between a circle of radius equal to ten (chord lengths) and the airfoil, is mapped into a rectangle in the transformed (ξ, η) plane. The airfoil and the circle are mapped into the lower and upper sides of the integration rectangle respectively and the two sides of an arbitrary cut, connecting the trailing edge of the airfoil to the outer circle, are mapped into the two vertical sides of the rectangle. In this way, the two vertical boundaries in the transformed plane correspond to the same physical line and, therefore, periodic

boundary conditions in the horizontal (ξ) direction are required. The transformation is provided by a set of two elliptic partial differential equations which are discretized and solved numerically by means of a point SOR method[6,7]. The step sizes in the transformed plane (ξ, η) are arbitrary, since they cancel out in the coordinate transformation finite difference equations, and are both taken equal to one, for convenience[6,7]. Further details are given in References 6 thru 10. The transformation of Thompson et al.[6,7] has been used satisfactorily in several numerical solutions of viscous and potential flows in regions containing any number of arbitrary two-dimensional bodies[8-10] and can be extended to three-dimensional configurations. Its two major limitations are due to the approximation introduced by imposing the free-stream boundary conditions at a finite distance from the body and to its inability of removing exactly sharp edge singularities. Whereas the boundary condition approximations are considered sufficient for the present study, the second limitation has been removed by considering an airfoil with a rounded trailing edge.

In the transformed coordinates the governing equations (1) and (2) become:

$$\omega_t + (\psi_\eta\, \omega_\xi - \psi_\xi\, \omega_\eta)/J - \Big(\frac{\alpha}{J^2}\,\omega_{\xi\xi} - \frac{2\beta}{J^2}\,\omega_{\xi\eta} + \frac{\gamma}{J^2}\,\omega_{\eta\eta} + \frac{\sigma}{J^2}\,\omega_\eta + \frac{\tau}{J^2}\,\omega_\xi\Big)/Re = 0 \tag{3}$$

and

$$\frac{\alpha}{J^2}\,\psi_{\xi\xi} - \frac{2\beta}{J^2}\,\psi_{\xi\eta} + \frac{\gamma}{J^2}\,\psi_{\eta\eta} + \frac{\sigma}{J^2}\,\psi_\eta + \frac{\tau}{J^2}\,\psi_\xi + \omega = \frac{\partial\psi}{\partial t}\,, \tag{4}$$

where J, α, β, γ, σ, τ are the Jacobian and the scale factors of the coordinate transformation, see Reference 10 for their analytical expressions.

The no-slip and zero injection boundary conditions at the surface of the airfoil are given in the transformed plane[8] as:

$$\psi\ (\xi,\ 0) = 0 \tag{5}$$

$$\psi_\eta(\xi,\ 0) = 0 \tag{6}$$

The free stream conditions, imposed on the circle enclosing the computational flow field, are:

$$\omega(\xi,\ \eta_M) = 0 \tag{7}$$

$$\psi(\xi,\ \eta_M) = y_c \cos\theta - x_c \sin\theta \tag{8}$$

where θ is the angle of attack of the free-stream flow, and x_c, y_c are the physical coordinates of the circle corresponding to ξ and η_M in the transformed plane, η_M being the height of the integration rectangle, equal to the number of gridpoints (in the η direction) minus one.

Finally, the coordinate transformation introduces the following additional (nonphysical) periodic boundary conditions:

$$\psi(\xi_M,\ \eta) = \psi(0,\ \eta) \tag{9}$$

and

$$\omega(\xi_M,\ \eta) = \omega(0,\ \eta) \tag{10}$$

where ξ_M is the width of the integration domain, equal to the number of gridpoints (in the ξ direction) minus one. As previously mentioned, boundary conditions (9) and (10) produce periodic two-by-two block tridiagonal systems in the second sweep of the ADI solution procedure. Such a difficulty has been resolved in the present study, where the Algorithm of Ahlberg et al.[18] for solving periodic tridiagonal system has been generalized to the use of periodic systems of two coupled tridiagonal equations (see the Appendix).

SECTION III

NUMERICAL METHOD

Equations (3) and (4) are expressed in finite difference form and solved numerically by means of the Douglas and Gunn[18] ADI procedure as follows: First, the nonlinear convective terms in the vorticity equation are (quasi)-linearized and the time derivative are replaced by finite differences to give:

$$(\omega^{n+1} - \omega^{n})/\Delta t + (\psi_{\eta}^{n+1}\,\omega_{\xi}^{n} + \psi_{\eta}^{n}\,\omega_{\xi}^{n+1} - \psi_{\eta}^{n}\,\omega_{\xi}^{n})/J$$

$$-(\psi_{\xi}^{n+1}\,\omega_{\eta}^{n} + \psi_{\xi}^{n}\,\omega_{\eta}^{n+1} - \psi_{\xi}^{n}\,\omega_{\eta}^{n})/J - (\alpha\,\omega_{\xi\xi}^{n+1} - 2\beta\,\omega_{\xi\eta}^{n}$$

$$+ \gamma\,\omega_{\eta\eta}^{n+1} + \sigma\,\omega_{\eta}^{n+1} + \tau\omega_{\xi}^{n+1})/Re = 0 \qquad (11)$$

and

$$\alpha\,\psi_{\xi\xi}^{n+1} - 2\beta\,\psi_{\xi\eta}^{n} + \gamma\,\psi_{\eta\eta}^{n+1} + \sigma\,\psi_{\eta}^{n+1} + \tau\psi_{\xi}^{n+1} + \omega^{n+1} = (\psi^{n+1} - \psi^{n})/\Delta t \qquad (12)$$

where the J^2 dividing α, β, γ, σ and τ has been omitted for convenience. Note that in equations (11) and (12) all the linear terms are expressed at the new time level $t^{n+1} = t^{n} + \Delta t$ implicitly except for the mixed derivatives which are expressed (explicitly) at the old time level t^{n}, see References 14 and 15. Alternatively, equations (3) and (4) can be linearized in time according to a Crank-Nicolson averaging to give:

$$(\omega^{n+1} - \omega^{n})/\Delta t + (\psi_{\eta}^{n+1}\,\omega_{\xi}^{n} + \psi_{\eta}^{n}\,\omega_{\xi}^{n+1})/2J - (\psi_{\xi}^{n+1}\,\omega_{\eta}^{n} + \psi_{\xi}^{n}\,\omega_{\eta}^{n+1})/2J$$

$$-[\frac{\alpha}{2}\,(\omega_{\xi\xi}^{n+1} + \omega_{\xi\xi}^{n}) - 2\beta\,\omega_{\xi\eta}^{n} + \frac{\gamma}{2}\,(\omega_{\eta\eta}^{n+1} + \omega_{\eta\eta}^{n})$$

$$+ \frac{\sigma}{2}\,(\omega_{\eta}^{n+1} + \omega_{\eta}^{n}) + \frac{\tau}{2}\,(\omega^{n+1} + \omega_{\xi}^{n})] = 0 \qquad (13)$$

and

$$\frac{\alpha}{2}\left(\psi_{\xi\xi}^{n+1}+\psi_{\xi\xi}^{n}\right)-2\beta\,\psi_{\xi\eta}^{n}+\frac{\gamma}{2}\left(\psi_{\eta\eta}^{n+1}+\psi_{\eta\eta}^{n}\right)+\frac{\sigma}{2}\left(\psi_{\eta\eta}^{n+1}+\psi_{\eta}^{n}\right)$$
$$+\frac{\tau}{2}\left(\psi_{\xi}^{n+1}+\psi_{\xi}^{n}\right)+\frac{\omega^{n+1}+\omega^{n}}{2}=\frac{\psi^{n+1}-\psi^{n}}{\Delta t} \tag{14}$$

which, except for the explicit mixed derivatives, are second order accurate in time. The two step ADI procedure of Douglas and Gunn[17] is then applied to equations (11) and (12) (or equivalently to equations (13) and (14)). In the first sweep, the solution (indicated by a *) is advanced in time by evaluating implicitly only the η derivatives and the source term (ω^{n+1}) in the stream function equation, and evaluating all the other terms at the old time level t^n. Equations (11) and (12) thus become:

$$\frac{\omega^*}{\Delta t}-\left(\frac{\psi_\xi^n}{J}+\frac{\sigma}{Re}\right)\omega_\eta^*-\frac{\gamma}{Re}\,\omega_{\eta\eta}^*+\frac{\omega_\xi^n}{J}\,\psi_\eta^*$$
$$=\frac{\omega^n}{\Delta t}+\left(\alpha\omega_{\xi\xi}^n-2\beta\omega_{\xi\eta}^n+\tau\omega_\xi^n\right)/Re \tag{15}$$

and

$$\omega^*-\frac{\psi^*}{\Delta t}+\sigma\psi_\eta^*+\gamma\psi_{\eta\eta}^*=-\frac{\psi^n}{\Delta t}-\tau\psi_\xi^n-\alpha\psi_{\xi\xi}^n+2\beta\psi_{\xi\eta}^n \tag{16}$$

Equation (15) and (16), after that all the derivatives are replaced with (second-order-accurate) central finite differences give a coupled set of linear tridiagonal equations of the type:

$$a1_j\,\omega_{j-1}^*+b1_j\,\omega_j^*+c1_j\,\omega_{j+1}^*+d1_j\,\psi_{j-1}^*+e1_j\,\psi_j^*+f1_j\,\psi_{j+1}^*=h1_j \tag{17}$$

and

$$a2_j\,\omega_{j-1}^*+b2_j\,\omega_j^*+c2_j\,\omega_{j+1}^*+d2_j\,\psi_{j-1}^*+e2_j\,\psi_j^*+f2_j\,\psi_{j+1}^*=h2_j \tag{18}$$

In equations (17) and (18) the subscript i (indicating the longitudinal ξ location) has been dropped for convenience, j varies from 2 to J-1 and all the coefficients are known and can be obtained straightforwardly from

equations (15) and (16). At all locations (i) equations (17) and (18) are solved very efficiently by Gauss block-tridiagonal reduction[16] thus providing all the $\omega^*_{i,j}$ and $\psi^*_{i,j}$ values ($i = 1,\ldots I$ and $j = 1,\ldots J$). Details of the boundary conditions will be provided later. In the second sweep of the ADI procedure, the final $(\psi^{n+1}, \omega^{n+1})$ solution is obtained by evaluating the ξ derivative and the source term ω^{n+1} (in equations 11 and 12) implicitly and the η derivatives explicitly from the first sweep * solution, that is:

$$\frac{\omega^{n+1}}{\Delta t} + \left(\frac{\psi^n_\eta}{J} - \frac{\tau}{Re}\right)\omega_\xi^{n+1} - \frac{\alpha}{Re}\,\omega^{n+1}_{\xi\xi} - \frac{\omega^n_\eta}{J}\,\psi^{n+1}_\xi$$

$$= -\frac{\omega^n_\xi}{J}\,(\psi^*_\eta - \psi^n_\eta) + \frac{\psi^n_\xi}{J}\,(\omega^*_\eta - \omega^n_\eta) + \frac{\omega^n}{\Delta t} + (\gamma\omega^*_{\eta\eta} + \sigma\omega^*_\eta$$

$$- 2\beta\,\omega^n_{\xi\eta})/Re \tag{19}$$

and

$$\omega^{n+1} + \tau\psi^{n+1}_\xi + \alpha\psi^{n+1}_{\xi\xi} - \psi^{n+1}/\Delta t = -\sigma\psi^*_\eta - \gamma\psi^*_{\eta\eta} + 2\beta\psi^n_{\xi\eta} - \psi^n/\Delta t \tag{20}$$

According to Briley and McDonald[12], equations (19) and (20) are replaced by the following ones obtained by subtracting equation (15) from (19) and (16) from (20), that is:

$$\frac{\bar{\omega}}{\Delta t} + \left(\frac{\psi^n_\eta}{J} - \frac{\tau}{Re}\right)\bar{\omega}_\xi - \frac{\alpha}{Re}\,\bar{\omega}_{\xi\xi} - \frac{\omega^n_\eta}{J}\,\bar{\psi}_\xi = \frac{\omega^* - \omega^n}{\Delta t} \tag{21}$$

and

$$\bar{\omega} + \tau\bar{\psi}_\xi + \alpha\bar{\psi}_{\xi\xi} - \frac{\bar{\psi}}{\Delta t} = -\frac{\psi^* - \psi^n}{\Delta t} + \omega^* - \omega^n \quad ,$$

where the new variables

$$\bar{\omega} = \omega^{n+1} - \omega^{n} \tag{23}$$

and

$$\bar{\psi} = \psi^{n+1} - \psi^{n} \tag{24}$$

have been introduced for convenience.

Equations (21) and (22), after that all the derivatives are replaced by central finite differences, become a set of coupled linear tridiagonal equations of the type

$$a1_i\ \bar{\omega}_{i-1} + b1_i\ \bar{\omega}_i + c1_i\ \bar{\omega}_{i+1} + d1_i\ \bar{\psi}_{i-1} + e1_i\ \bar{\psi}_i + f1_i\ \bar{\omega}_{i+1} = h1_i \tag{25}$$

and

$$a2_i\ \bar{\omega}_{i-1} + b2_i\ \bar{\omega}_i + c2_i\ \bar{\omega}_{i+1} + d2_i\ \bar{\psi}_{i-1} + e2_i\ \bar{\psi}_i + f2_i\ \bar{\psi}_{i+1} = h2_i, \tag{26}$$

where the subscript j is now dropped for convenience and all the $a1_i$ thru $h2_i$ coefficients are known. Equations (25) and (26) constitute, for $i = 1,\ldots I$, a system of 2I coupled tridiagonal equations subject to periodic boundary conditions, so that for $i = 1$, $\bar{\omega}_{i-1}$ and $\bar{\psi}_{i-1}$ are replaced by $\bar{\omega}_I$ and $\bar{\psi}_I$ and for $i = I$, ω_{i+1} and ψ_{i+1} are replaced by $\bar{\omega}_1$ and $\bar{\psi}_1$. This system is solved very efficiently by means of the algorithm presented in the Appendix for all rows, i.e., for $j = 2,\ldots J - 1$. It is worth noting that the $\omega^*_{i,j}$ and $\psi^*_{i,j}$ values appearing in the coefficients $h1_j$ and $h2_j$ are not needed for the evaluation of $\bar{\omega}_{i,j}$ and $\bar{\psi}_{i,j}$ in any successive row. Therefore, the same arrays are used to store $\omega^*_{i,j}$ and $\bar{\omega}_{i,j}$ and $\psi^*_{i,j}$ and $\bar{\psi}_{i,j}$.

The solution at the new t^{n+1} time can now be evaluated as:

$$\omega^{n+1}_{i,j} = \omega^{n}_{i,j} + \bar{\omega}_{i,j} \tag{27a}$$

and

$$\psi^{n+1}_{i,j} = \psi^{n}_{i,j} + \bar{\psi}_{i,j} \tag{27b}$$

for $i = 1,\dots I$ and $j = 2,\dots J - 1$ and as

$$\omega_{i,j}^{n+1} = \omega_{i,j}^{*} \tag{28a}$$

and

$$\psi_{i,j}^{n+1} = \psi_{i,j}^{*} \tag{28b}$$

for $i = 1,\dots I$ and $j = 1$ or $j = J$.

The whole process is then repeated until convergence.

A. Boundary Conditions for the * Solution

In the first sweep of the numerical procedure equations (17) and (18) have to be solved at every longitudinal location, subject to boundary conditions (5-8).

Equations (5), (7) and (8) are immediately imposed as

$$\psi_1^* = 0 \tag{29}$$

$$\psi_J^* = 0 \tag{30}$$

$$\omega_J^* = 0 \tag{31}$$

Equation (6) can be satisfied in several different ways. The following five approaches were used in the present study. Three, four and five-point one-sided finite difference representations of equation (6) give respectively (the step size is equal to one and ψ_1^* is eliminated due to equation (29)):

$$\psi_3^* = 4\psi_2^* \tag{32}$$

$$\psi_4^* = (9\psi_3^* - 18\psi_2^*)/2 \tag{33}$$

$$\psi_5^* = \frac{16}{3}\,\psi_4^* - 12\psi_3^* + 16\psi_2^* \tag{34}$$

For the case of Cartesian coordinates ($\eta \equiv y$, $\gamma \equiv 1$, $\sigma \equiv 0$) a linear shear flow was also assumed near the body surface[19] which gives the following equation:

$$\omega_1^* + \frac{1}{2}\omega_2^* + 3\psi_2^* = 0 \tag{35}$$

Finally, a central finite difference for ψ_η^* was used, consistently with the overall numerical procedure, i.e.,

$$\psi_2^* - \psi_0^* = 0 \tag{36}$$

However, the value of ψ_0^*, interior to the body was not available and had to be evaluated somehow. To this purpose the steady state stream function equation along the $\eta = 0$ ($j = 1$) line, where all the ξ derivatives vanish identically, is easily seen to provide

$$\gamma\psi_{\eta\eta}^* + \omega^* = 0 \ , \tag{37}$$

which, in finite difference form, becomes

$$\gamma_1(\psi_2^* - 2\psi_1^* + \psi_0^*) + \omega_1^* = 0 \tag{38}$$

This, combined with equations (29) and (36) finally gives

$$2\gamma_1^*\psi_2^* + \omega_1^* = 0 \tag{39}$$

where γ_1 is evaluated by a three-point extrapolation from γ_2, γ_3 and γ_4. Any of equations (32) thru (35) or (39) is easily satisfied in the block tridiagonal inversion of equations (17) and (18). Such an inversion is similar to, and simpler than, that given in the Appendix. In particular, it provides recursion relations of the type

$$\omega_j^* = R1_j\ \omega_{j-1}^* + S1_j\ \psi_{j-1}^* + T1_j \tag{40}$$

$$\psi_j^* = R2_j\ \omega_{j-1}^* + S2_j\ \psi_{j-1}^* + T2_j \ , \tag{41}$$

where $R1_j$ thru $T2_j$ are given in terms of $R1_{j+1}$ thru $T2_{j+1}$ and can be easily determined for $j = J - 1, J - 2, \ldots, 2$ since, from boundary conditions (30) and (31):

$$R1_J = = S1_J = T1_J = R2_J = S2_J = T2_J = 0 \tag{42}$$

Any of equations (32) thru (35) or (39), together with (40) and (41) easily provides a relation for ω_1^* in terms of known coefficients, and all ω_j^* and ψ_j^* can finally be evaluated by means of the recursion formulas (40) and (41).

SECTION IV

RESULTS

The present numerical technique was applied to three different problems: a simple Poiseuille Flow, for which the second order accuracy of the method could be verified versus the exact analytical solution; the driven cavity problem for which a fully two-dimensional solution could be compared with available numerical results and finally flow past a NACA 0012 airfoil in order to assess the capability of the present method to achieve its goal of computing arbitrary two-dimensional flow fields.

A. Poiseuille Flow

For laminar steady flow inside a two dimensional channel, at any location x, the longitudinal velocity profile is parabolic and the normal velocity is zero everywhere. For convenience, the maximum velocity at the center of the channel (y = h) was taken to be equal to h. The exact analytical solutions for the vorticity and the stream function in the lower half of the channel ($0 \leq y \leq h$) are therefore given as:

$$\omega = -2 + 2\frac{y}{h} \tag{43}$$

and

$$\psi = y^2 - \frac{y^3}{3h} \tag{44}$$

Two numerical solutions were obtained by using 5 gridpoints in the longitudinal x ($x \equiv \xi$) direction and 11 and 21 points in the normal y ($y \equiv \eta$) direction, so that h was equal to 10 and 20 respectively ($\Delta y \equiv 1$). The one dimensional nature of the solution was captured perfectly thanks to the periodic boundary conditions in the ξ direction. The vorticity at the wall was found to be equal to - 1.9900 and -1.9975 (for 11 and 21 gridpoints respectively), when using the point image boundary condition of Burggraf[1],

equation (39), ($\gamma_1 \equiv 1$, for this case) thus verifying the second order accuracy of the method. The other four boundary conditions for $\psi_y = \psi_\eta = 0$ at the wall were also used and found totally satisfactory. Actually, equations (33), (34) and (35) all replicated the exact (analytical) results. It was mentioned that an "implicit" and a Crank Nicolson time splitting of the governing equations could be used, see equations (11) thru (14); both approaches have been implemented, found to be unconditionally stable for this model problem and have produced, at convergence, identical results.

B. Driven Cavity Problem

The present algorithm was also applied to the classical square cavity problem[1]. For this case the boundary conditions are nonperiodic in both x and y directions. The stream function ψ is prescribed to be zero on all walls of the unit square flow field and the derivative of ψ in the direction normal to the wall is equal to one on the top side of the square and to zero on the remaining three sides. These homogeneous boundary conditions in the x direction have been accommodated in the present incremental formulation for $\bar{\psi}$ and $\bar{\omega}$ in the second sweep of the ADI procedure. The point image approach of Burggraf[1] has been used for these derivative boundary conditions and was again found to be very satisfactory. Results were obtained with 30 step sizes in either x and y directions, for a value of the Reynolds Number of 100. They are presented in figures 1 and 2 as the horizontal velocity profile thru the gridpoint characterized by the maximum (absolute) value of the stream function, and the contour plot of the stream function itself. In figure 1 the results of Rubin et al.[20,22] obtained by means of a spline approach using 28 by 28 meshes in each direction are shown for comparison.

The agreement is satisfactory and provides further evidence of the correctness of the present approach. No quantitative comparison is given in figure 2, where the stream function contours correspond to values of -0.01, -0.015, -0.020....-0.095 and agree reasonably well in values and shape with previously published results[1,22].

C. Flow Past a NACA 0012 Airfoil

Flow past a NACA 0012 airfoil was finally considered in order to test the present numerical technique in combination with the transformation of Thompson et al.[6,7]. In order to avoid the difficulties associated with a sharp trailing edge, this has been smoothed by means of a circular arc, see figures 3 and 4 which also provide the transformed coordinate lines in the physical plane. The coordinate transformation, as used in the present study, has been kindly provided by Captain H. A. Hegna[21] who has optimized the spacing of the (η = constant) coordinate lines near the body surface for turbulent flow at a value of the Reynolds number of about 10^5. No attempt was made in the present study at optimizing the above mentioned coordinate spacing for the present laminar flow calculations. Figure 3 clearly shows the outer boundary of the integration domain in the physical plane, that is, a circle of center in the origin and radius equal to 10. The body and the coordinate lines immediately around it are instead very poorly resolved by the large scale of the computer plot. Figure 4 shows a blow-up of the airfoil whose nondimensional chord length equals 1 and of the coordinate lines immediately surrounding it. However, even such a fairly large scale is not sufficient to clearly show the spacing of the η = constant coordinate lines immediately surrounding the airfoil.

Solutions have been obtained for flow at zero angle of attack for two values of the Reynolds number, namely $Re = 10^2$ and $Re = 10^4$. The corresponding velocity vector plots are given in figures 5 and 6, respectively. Figure 5 shows a typical attached viscous flow configuration with a clearly visible boundary layer near the surface of the body. In figure 6, the higher Reynolds number is clearly seen to produce a much thinner boundary layer. A blow-up of the velocity distribution, very close to the body surface, is given in figures 7 and 8 for the same two flow configurations. These figures clearly show that despite a coordinate spacing independent of the Reynolds number, the numerical solution has been able to capture the shrinking of the boundary layer thickness with increasing Reynolds number of the flow. It is obvious, however, that an optimization of the coordinate spacing is warranted in order to obtain highly accurate solutions at Reynolds number values of 10^4 or higher. A $Re = 10^2$ flow at an angle of attack of 0.1 has also been computed and the results are given in figure 9 again as velocity vectors. Separated flows were not attempted due to the fact that all convective terms in the governing equations are represented by central finite differences. However, first order accurate windward finite difference representations for such terms can be easily accommodated in the present algorithm. The present approach is computationally very fast insofar as the solution proceeds thru 100 time steps within about 2 CPU minutes of CDC Cyber 175 for the present calculations employing a grid of 70 by 44 points. The method of Thompson et al[8] requires a comparable amount of computer time for advancing the solution of a single time step. However, the convergence rate was found to be lower than anticipated: whereas, for the driven cavity problem 150 time steps

($\Delta t = .1$) were sufficient for a satisfactory convergence ($[(\omega^{n+1} - \omega^{n})/\omega^{n}]_{\text{average}} < 10^{-5}$), for the flow past the NACA 0012 airfoil the relative error in the solution was still of the order of 10^{-4}, after 200 time cycles. Further, in order to obtain convergence, the solution had to be started with a very small step size ($\Delta t = 10^{-4}$), which was then increased at every iteration by a factor of 1.1, until a value of 10^{-2} was reached, and was then kept constant at that value, in order to avoid divergence. All results have been obtained with the backward-in-time approach. The program using a Crank Nicolson averaging was not found to converge for comparable values of the time step.

SECTION V

CONCLUSIONS AND RECOMMENDATIONS

An algorithm for solving the vorticity-stream function Navier-Stokes equations for steady laminar flow past an arbitrary airfoil has been developed. The governing equations are written in a system of body oriented coordinates[6,7] and solved by means of the ADI procedure of Douglas and Gunn[17]. The present approach has computed the flow field past a NACA 0012 airfoil successfully, and has shown to be cost-competitive with other approaches available in the technical literature. Further, it could be easily modified to extend its capability to unsteady flow computations by relaxing the stream function equation at every time step by any suitable numerical technique (line SOR, ADI, Direct solvers). However, the present approach needs improvements with respect to the convergence rate and the present inability to compute separated flows. In this respect, the effect of windward differencing and variable time steps[4,13] is certainly worth investigating. Finally, it is the author's belief that further, dramatic improvements could be obtained by incorporating the very promising multi-grid idea of Brandt[23].

REFERENCES

1. O. R. Burggraf, "Analytical and Numerical Studies of the Structure of Steady Separated Flows," J. Fluid Mech. (1966) Vol. 24, part 1 pp. 113-151.

2. R. T. Davis, "Numerical Solution of the Navier-Stokes Equations for Symmetric Laminar Incompressible Flow Past a Parabola," J. Fluid Mech. (1972) Vol. 51, part 3, pp. 417-433.

3. U. Ghia and R. T. Davis, "Solutions of Navier-Stokes Equations for Flow Past a Class of Two-Dimensional Semi-Infinite Bodies," AIAA Journal, Vol. 12, no. 12, December 1974.

4. M. Napolitano, M. J. Werle and R. T. Davis, "Numerical Solutions for High Reynods Number Separated Flow Past a Semi-Infinite Compression Corner," Computers and Fluids (1979) Vol. 7, pp. 165-175.

5. U. B. Mehta and Z. Lavan, "Starting Vortex, Separation Bubbles and Stall: A Numerical Study of Laminar Unsteady Flow Around an Airfoil," J. Fluid Mech. (1975), Vol. 67, part 2, pp. 227-256.

6. J. F. Thompson, F. C. Thames and C. W. Mastin, "Automatic Numerical Generation of Body Fitted Curvilinear Coordinate System for Fields Containing Any Number of Arbitrary Two-Dimensional Bodies," J. Computational Phys., Vol. 15 (1974) p. 299.

7. J. F. Thompson, F. C. Thames and C. W. Mastin, "TOMCAT - A Code for Numerical Generation of Boundary Fitted Curvilinear Coordinate Systems on Fields Containing Any Number of Arbitrary Two-Dimensional Bodies," J. Computational Phys., Vol. 24 (1977) pp. 274-302.

8. F. C. Thames, J. F. Thompson, C. W. Mastin and R. L. Walker, "Numerical Solutions for Viscous and Potential Flow about Arbitrary Two-Dimensional Bodies Using Body-Fitted Coordinate Systems," J. Computational Phys., Vol. 24 (1977) pp. 245-273.

9. J. F. Thompson, F. C. Thames, J. K. Hodge, S. P. Shanks, R. N. Reddy and C. W. Mastin, "Solutions of the Navier-Stokes Equations in Various Flow Regimes on Fields Containing Any Number of Arbitrary Bodies Using Boundary-Fitted Coordinate Systems," Proceedings of the Fifth International Conference on Numerical Methods in Fluid Dynamics, Lecture Notes in Physics, Vol. 59 (1976) Springer Verlag, pp. 421-427.

10. J. K. Hodge, A. L. Stone, T. E. Miller, "Numerical Solutions for Airfoils near Stall in Optimized Boundary-Fitted Curvilinear Coordinates," AIAA Journal, Vol. 17, no. 5, May 1979, pp. 458-464.

11. W. R. Briley, "A Numerical Study of Laminar Separated Bubbles Using the Navier-Stokes Equations," J. Fluid Mech. (1971) Vol. 47, part 4, pp. 713-736.

12. W. R. Briley and H. McDonald, "Solution of the Multidimensional Compressible Navier-Stokes Equations by a Generalized Implicit Method," J. Computational Phys. Vol. 24 (1977) pp. 372-397.

13. W. R. Briley and H. McDonald, "On the Structure and Use of Linearized Block ADI and Related Schemes," J. Computational Phys., to be published.

14. R. M. Beam and F. F. Warming, "An Implicit Factored Scheme for the Compressible Navier-Stokes Equations," AIAA Journal, Vol. 16, no. 4, April 1978, pp. 393-402.

15. J. A. Hill, R. T. Davis and G. L. Slater, "Development of a Factored ADI Scheme for Solving the Navier-Stokes Equations in Stream Function Vorticity Variables," University of Cincinnati, AFL Report, no. 79-12-48, Dept of Aero Engineering and Applied Mechanics, December 1979.

16. E. Isacson and H. B. Keller, "Analysis of Numerical Methods," Wiley, New York, 1966.

17. J. Douglas and J. E. Gunn, "A General Formualtion of Alternating Direction Methods," Numerische Matematik, Vol. 6 (1964) pp. 428-453.

18. H. H. Ahlberg, E. N. Nilson and J. L. Walsh, "The Theory of Splines and Their Applications," Academic Press, New York, 1967.

19. M. Atias, M. Wolfshtein and M. Israeli, "Efficiency of Navier-Stokes Solvers," AIAA J., Vol. 15, no. 2, February 1977, pp. 263-266.

20. S. G. Rubin and P. K. Khosla, Polynomial Interpolation Methods for Viscous Flow Calculations," J. Computational Phys., Vol. 24 (1977) pp. 217-244.

21. H. A. Hegna, "Numerical Solution of Incompressible Turbulent Flow Over Airfoils," Ph.D. Dissertation, Air Force Institute of Technology, Dayton, Ohio, 1980.

22. S. G. Rubin et al. "Numerical Studies of Incompressible Viscous Flow in a Driven Cavity," NASA SP 378, 1975.

23. A. Brandt, "Multi-Level Adaptive Computations in Fluid Dynamics, AIAA Paper 79-1455, AIAA Computational Fluid Dynamics Conference, Williamsburg, Va., July 23-25, 1979.

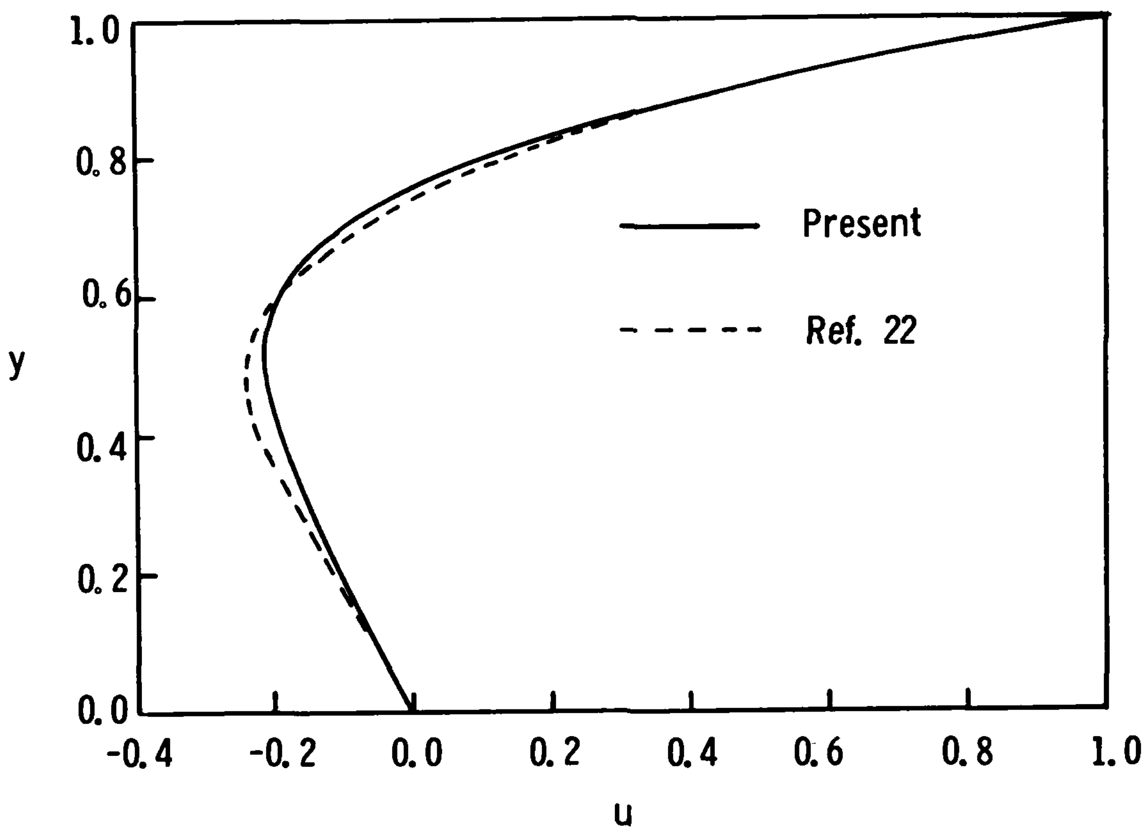

Figure 1. Driven Cavity; Re=100 Longitudinal Velocity Profile Thru ψ_{max}

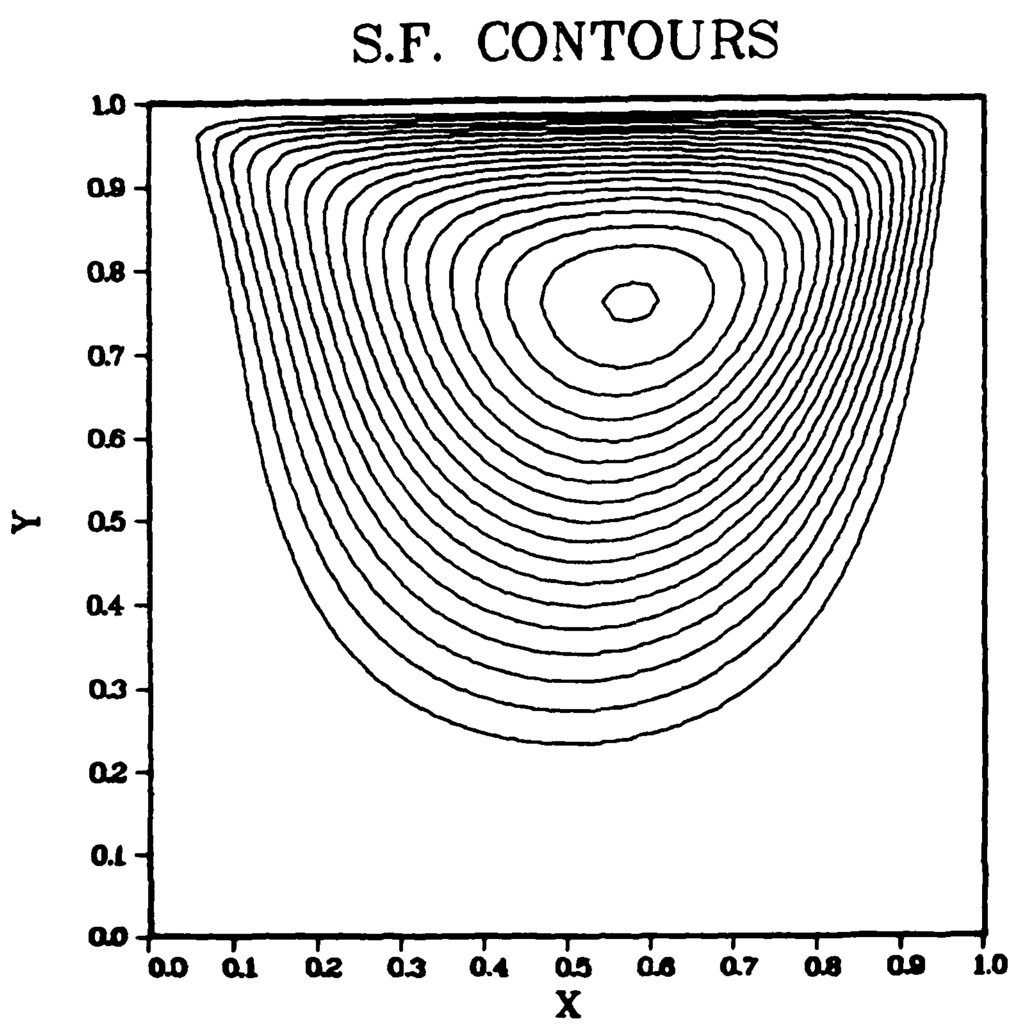

Figure 2. Driven Cavity; Re=100 Stream Function Contour Plot

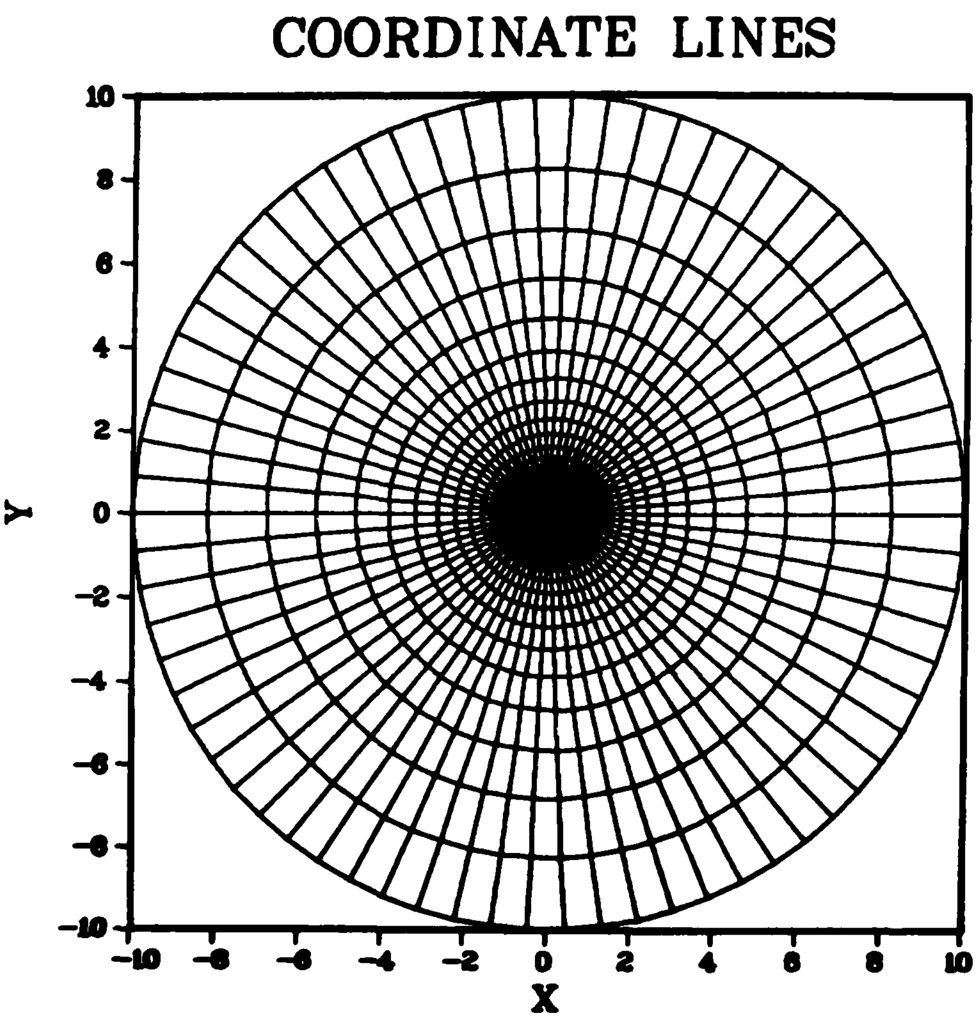

Figure 3. NACA 0012 Airfoil; Body-Oriented Coordinates (Far Field)

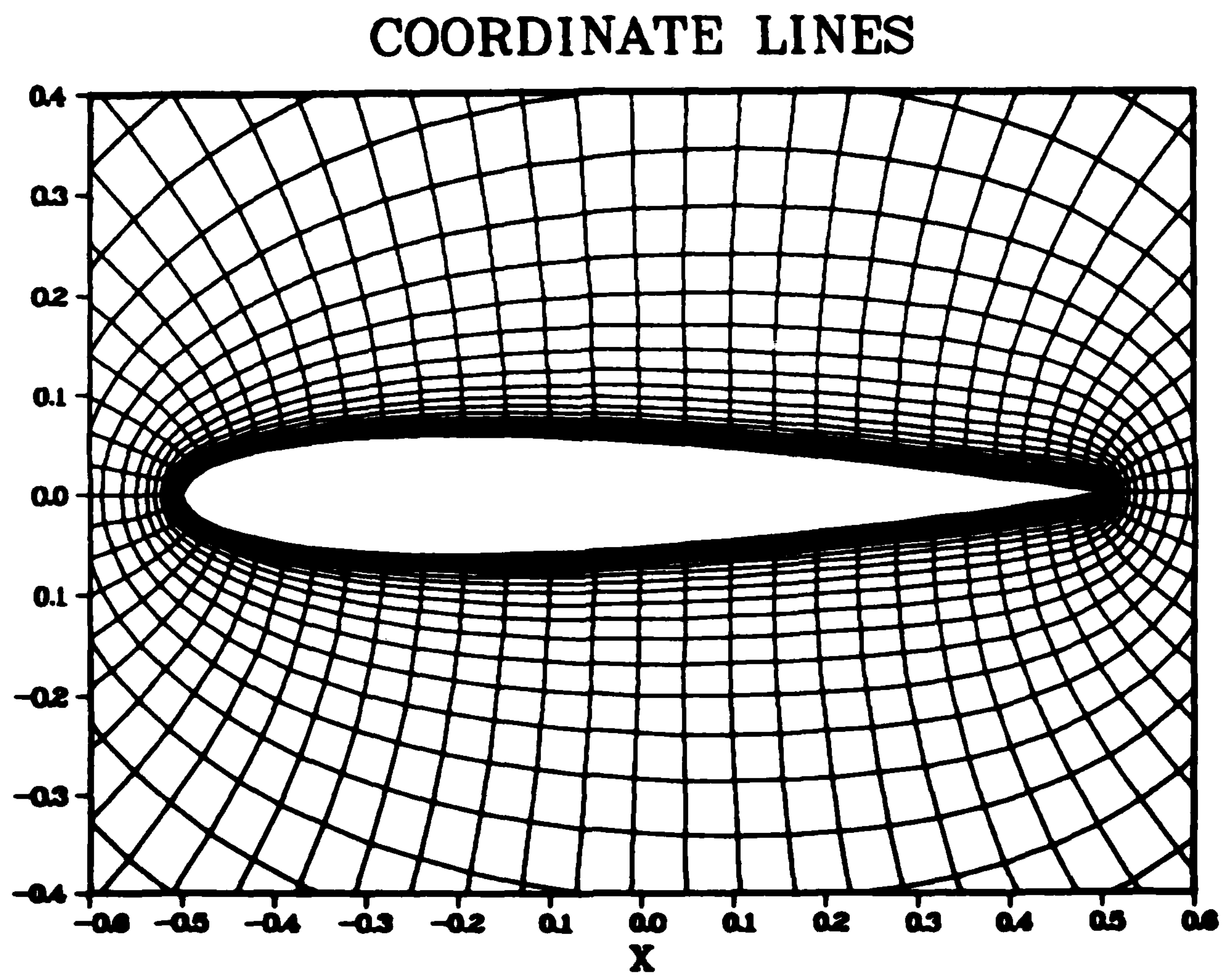

Figure 4. NACA 0012 Airfoil; Body-Oriented Coordinates (Near Field)

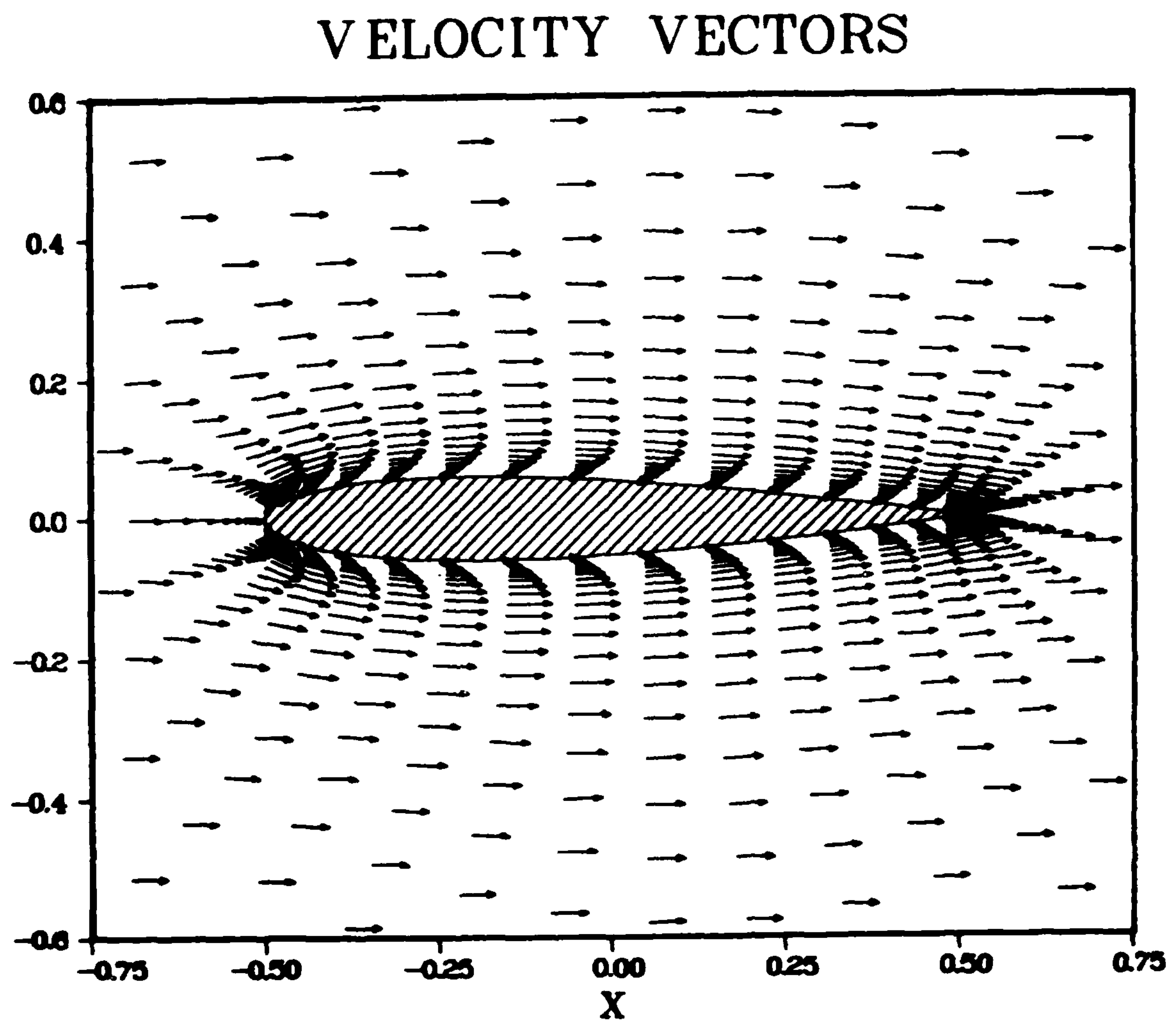

Figure 5. NACA 0012 Airfoil; Re=100 Velocity Vectors

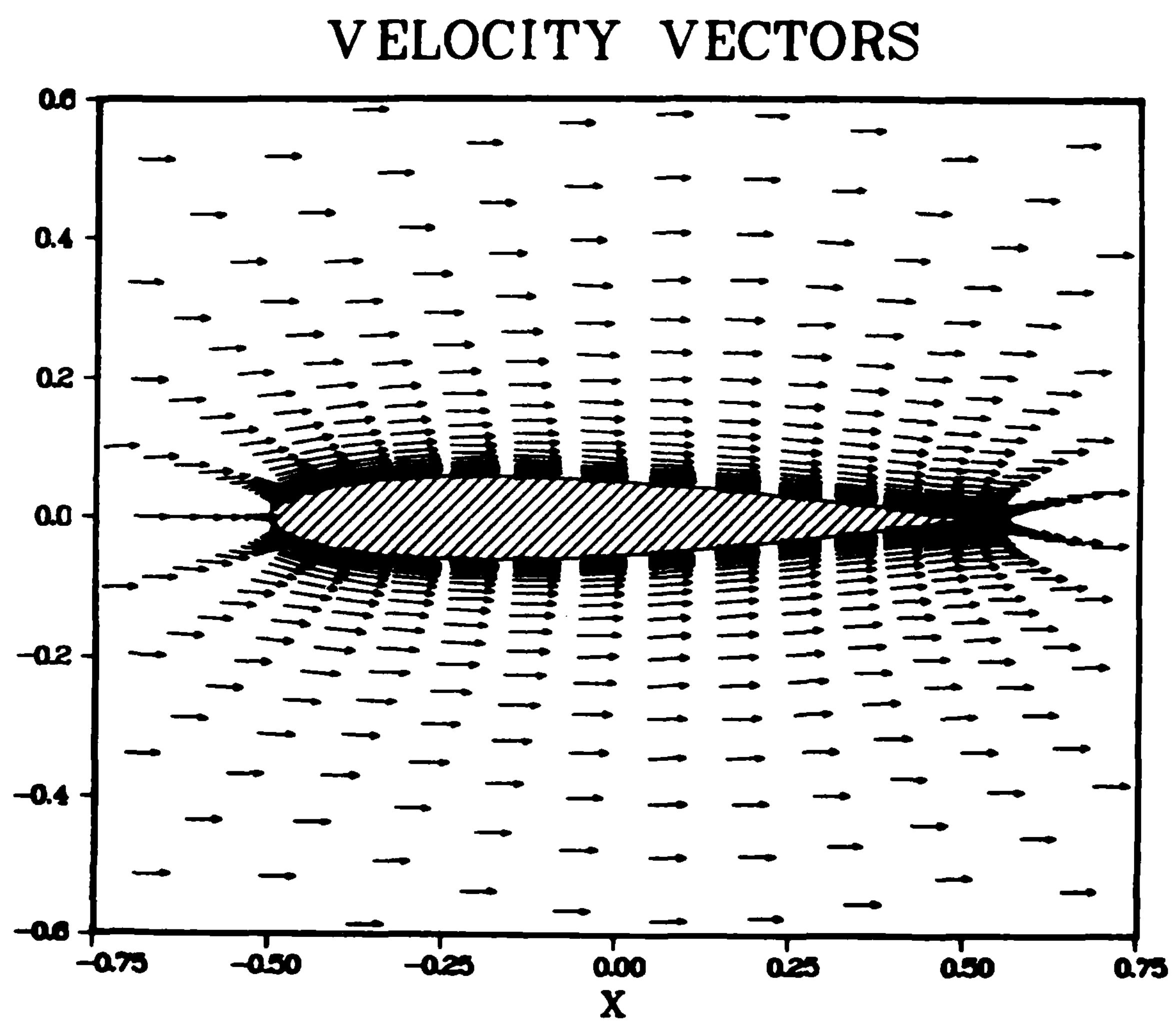

Figure 6. NACA 0012 Airfoil; Re=10,000 Velocity Vectors

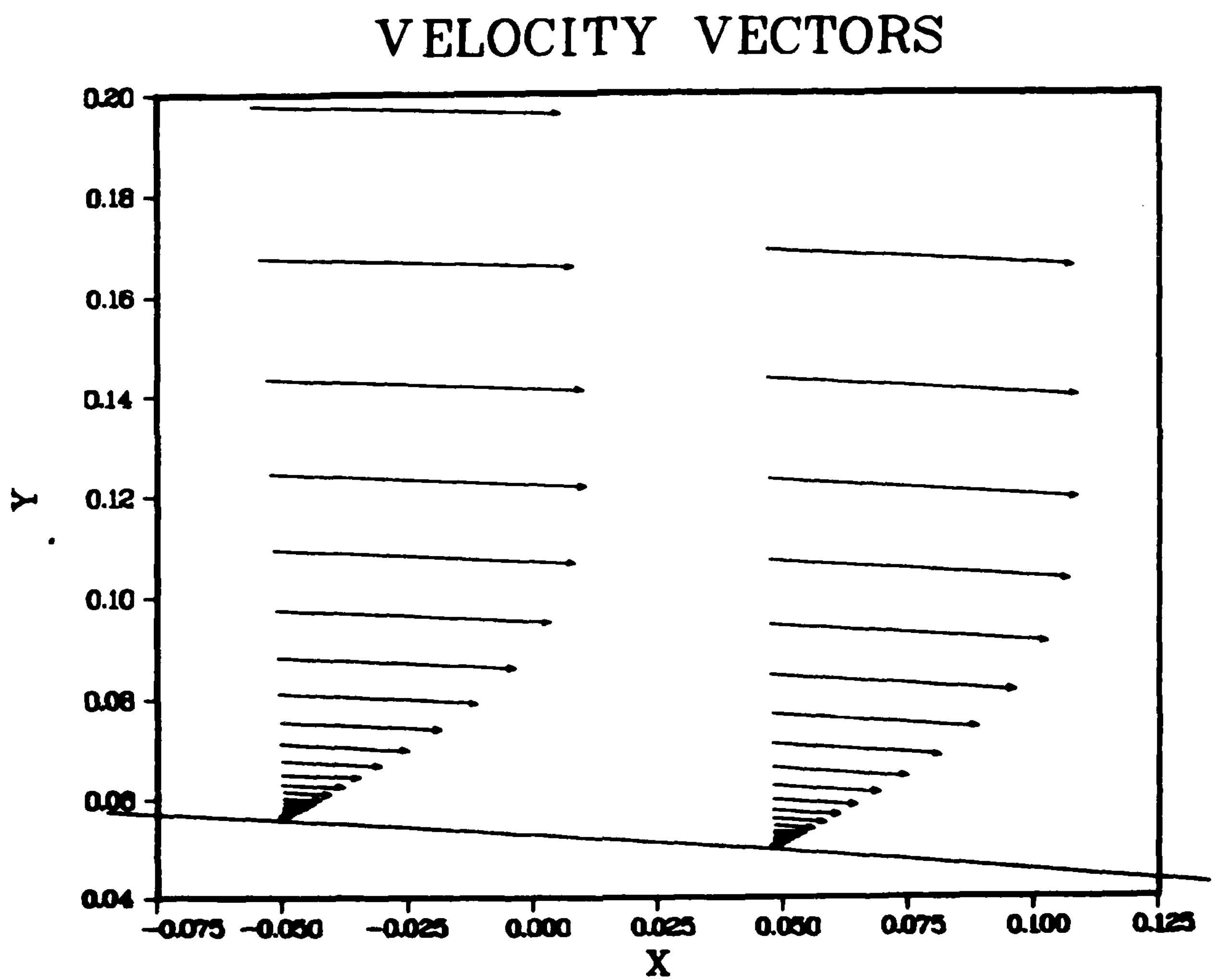

Figure 7. NACA 0012 Airfoil; Re=100 Boundary Layer Profiles

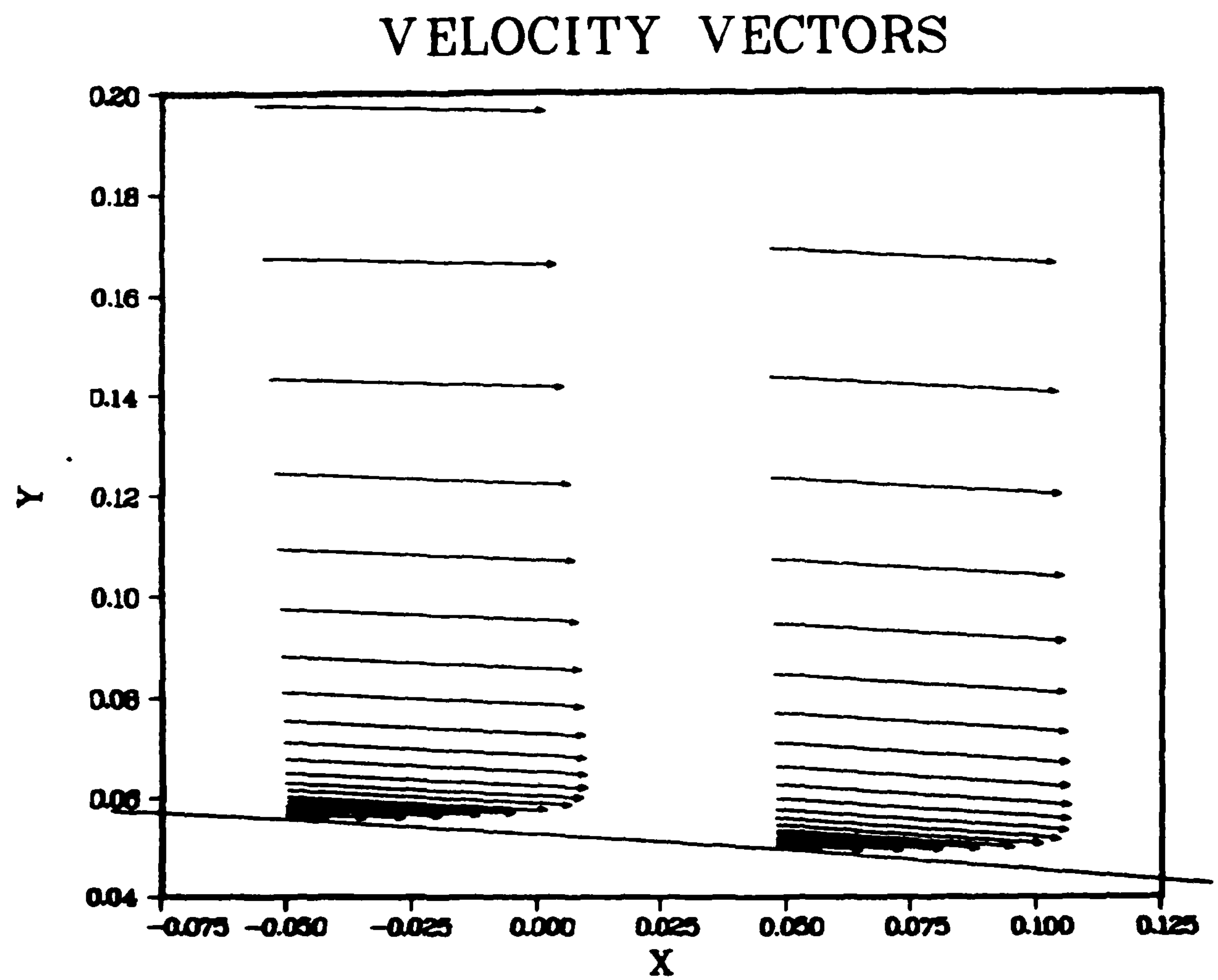

Figure 8. NACA 0012 Airfoil; Re=10,000 Boundary Layer Profiles

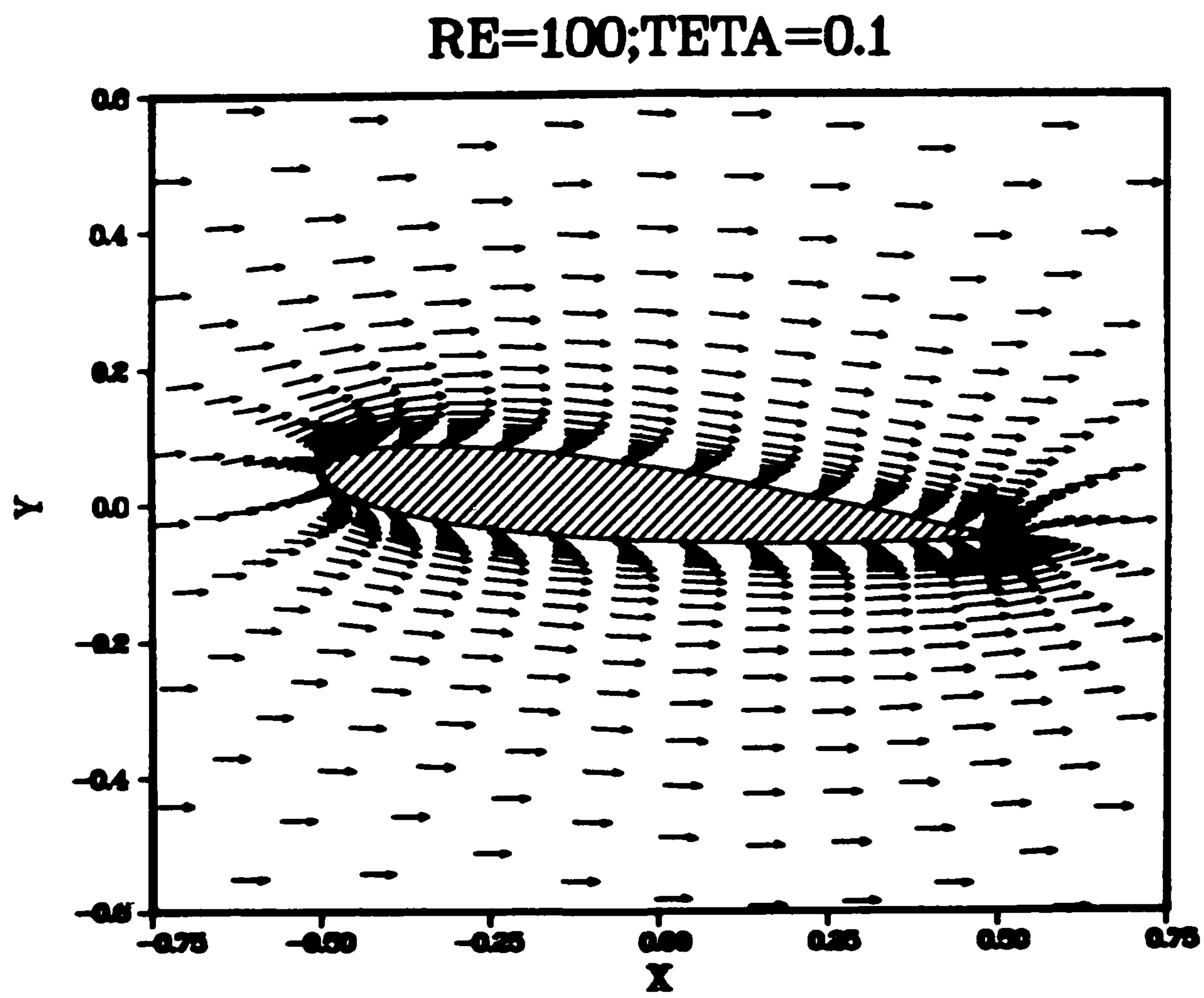

Figure 9. NACA 0012 Airfoil; Re=100 Flow At θ = 0.1 Angle of Attack

APPENDIX

AN ALGORITHM FOR THE SOLUTION OF PERIODIC SYSTEMS OF TWO COUPLED TRIDIAGONAL EQUATIONS

Algorithm

The present Appendix generalizes the algorithm of Ahlberg et al.[18], for solving tridiagonal periodic systems, to the case of two-by-two block tridiagonal systems.

The most general tridiagonal system for 2I coupled equations in 2I unknowns k_i, F_i, $i = 1, 2 \ldots I$, with periodic boundary conditions is given as:

$$a1_1\ k_I + b1_1\ k_1 + c1_1\ k_2 + d1_1\ F_I + e1_1\ F_1 + f1_1\ F_2 = h1_1 \tag{1a}$$

$$a2_1\ k_I + b2_1\ k_1 + c2_1\ k_2 + d2_1\ F_I + e2_1\ F_1 + f2_1\ F_2 = h2_1 \tag{1b}$$

$$\ldots\ldots\ldots\ldots\ldots\ldots\ldots\ldots\ldots$$

$$a1_i\ k_{i-1} + b1_i\ k_i + c1_i\ k_{i+1} + d1_i\ F_{i-1} + e1_i\ F_i + f1_i\ F_{i+1} = h1_i \tag{2a}$$

$$a2_i\ k_{i-1} + b2_i\ k_i + c2_i\ k_{i+1} + d2_i\ F_{i-1} + e2_i\ F_i + f2_i\ F_{i+1} = h2_i \tag{2b}$$

$$\ldots\ldots\ldots\ldots\ldots\ldots\ldots\ldots\ldots\ldots\ldots$$

$$a1_I\ k_{I-1} + b1_I\ k_I + c1_I\ k_1 + d1_I\ F_{I-1} + e1_I\ F_I + f1_I\ F_1 = h1_I \tag{3a}$$

$$a2_I\ k_{I-1} + b2_I\ k_I + c2_I\ k_1 + d2_I\ F_{I-1} + e2_I\ F_I + f2_I\ F_1 = h2_I. \tag{3b}$$

Let us assume the following recursion relations for the unknowns, k_i, F_i:

$$k_i = r1_i\ k_{i+1} + s1_i\ F_{i+1} + t1_i + u1_i\ k_I + v1_i\ F_I\ , \tag{4a}$$

$$F_i = r2_i\ k_{i+1} + s2_i\ F_{i+1} + t2_i + u2_i\ k_I + v2_i\ F_I\ . \tag{4b}$$

Equations (4a) and (4b) are valid for any value of i. They can be used, therefore, to eliminate k_{i-1} and F_{i-1} from equations (2a,b), which become:

$$\overline{b1}_i\ k_i + \overline{c1}_i\ k_{i+1} + \overline{e1}_i\ F_i + \overline{f1}_i\ F_{i+1} + \overline{m1}_i\ k_I + \overline{n1}_i\ F_I = \overline{h1}_i\ , \tag{5a}$$

$$\overline{b2}_i\ k_i + \overline{c2}_i\ k_{i+1} + \overline{e2}_i\ F_i + \overline{f2}_i\ F_{i+1} + \overline{m2}_i\ k_I + \overline{n2}_i\ F_I = \overline{h2}_i\ , \tag{5b}$$

with:

$$\overline{b1}_i = a1_i\ r1_{i-1} + d1_i\ r2_{i-1} + b1_i\ , \tag{6a}$$

$$\overline{c1}_i = c1_i\ , \tag{7a}$$

$$\overline{e1}_i = a1_i\ s1_{i-1} + d1_i\ s2_{i-1} + e1_i\ , \tag{8a}$$

$$\overline{f1}_i = f1_i\ , \tag{9a}$$

$$\overline{m1}_i = a1_i\ u1_{i-1} + d1_i\ u2_{i-1}\ , \tag{10a}$$

$$\overline{n1}_i = a1_i\ v1_{i-1} + d1_i\ v2_{i-1}\ , \tag{11a}$$

$$\overline{h1}_i = h1_i - a1_i\ t1_{i-1} - d1_i\ t2_{i-1}\ , \tag{12a}$$

and:

$$\overline{b2}_i = a2_i\ r1_{i-1} + d2_i\ r2_{i-1} + b2_i\ , \tag{6b}$$

$$\overline{c2}_i = c2_i\ , \tag{7b}$$

$$\overline{e2}_i = a2_i\ s1_{i-1} + d2_i\ s2_{i-1} + e2_i\ , \tag{8b}$$

$$\overline{f2}_i = f2_i\ , \tag{9b}$$

$$\overline{m2}_i = a2_i\ u1_{i-1} + d2_i\ u2_{i-1}\ , \tag{10b}$$

$$\overline{n2}_i = a2_i\ v1_{i-1} + d2_i\ v2_{i-1}\ , \tag{11b}$$

$$\overline{h2}_i = h2_i - a2_i\ t1_{i-1} - d2_i\ t2_{i-1}, \tag{12b}$$

The rl_i thru tl_i coefficients can now be determined by multiplying equations (5a) and (5b) by $\overline{e2}_i$ and $\overline{el}_i$ respectively, subtracting them to eliminate F_i and solving for k_i, to give:

$$rl_i = (\overline{el}_i\ \overline{c2}_i - \overline{e2}_i\ \overline{cl}_i)/(\overline{bl}_i\ \overline{e2}_i - \overline{b2}_i\ \overline{el}_i), \tag{13a}$$

$$sl_i = (\overline{el}_i\ \overline{f2}_i - \overline{e2}_i\ \overline{fl}_i)/(\overline{bl}_i\ \overline{e2}_i - \overline{b2}_i\ \overline{el}_i), \tag{14a}$$

$$ul_i = (\overline{el}_i\ \overline{m2}_i - \overline{e2}_i\ \overline{ml}_i)/(\overline{bl}_i\ \overline{e2}_i - \overline{b2}_i\ \overline{el}_i), \tag{15a}$$

$$vl_i = (\overline{el}_i\ \overline{n2}_i - \overline{e2}_i\ \overline{nl}_i)/(\overline{bl}_i\ \overline{e2}_i - \overline{b2}_i\ \overline{el}_i), \tag{16a}$$

$$tl_i = (\overline{e2}_i\ \overline{hl}_i - \overline{el}_i\ \overline{h2}_i)/(\overline{bl}_i\ \overline{e2}_i - \overline{b2}_i\ \overline{el}_i). \tag{17a}$$

The $r2_i$ thru $t2_i$ coefficients are similarly obtained by elminating k_i and solving for F_i to give:

$$r2_i = (\overline{bl}_i\ \overline{c2}_i - \overline{b2}_i\ \overline{cl}_i)/(\overline{el}_i\ \overline{b2}_i - \overline{e2}_i\ \overline{bl}_i), \tag{13b}$$

$$s2_i = (\overline{bl}_i\ \overline{f2}_i - \overline{b2}_i\ \overline{fl}_i)/(\overline{el}_i\ \overline{b2}_i - \overline{e2}_i\ \overline{bl}_i), \tag{14b}$$

$$u2_i = (\overline{bl}_i\ \overline{m2}_i - \overline{b2}_i\ \overline{ml}_i)/(\overline{el}_i\ \overline{b2}_i - \overline{e2}_i\ \overline{bl}_i), \tag{15b}$$

$$v2_i = (\overline{bl}_i\ \overline{n2}_i - \overline{b2}_i\ \overline{nl}_i)/(\overline{el}_i\ \overline{b2}_i - \overline{e2}_i\ \overline{bl}_i), \tag{16b}$$

$$t2_i = (\overline{b2}_i\ \overline{hl}_i - \overline{bl}_i\ \overline{h2}_i)/(\overline{el}_i\ \overline{b2}_i - \overline{e2}_i\ \overline{bl}_i). \tag{17b}$$

The rl_I thru $t2_i$ coefficients are evaluated by means of equations (1a,b) in the same way and all the rl_i thru $t2_i$ (i=2...,I-1) can then be evaluated by means of equations (13a-17b). In order to evaluate the F_i and k_i unknowns (i.e. to solve the original system of equations) let us now take:

$$k_i = wul_i\ k_I + wvl_i\ F_I + wtl_i, \tag{18a}$$

$$F_i = wu2_i\ k_I + wv2_i\ F_I + wt2_i, \tag{18b}$$

with the $wu1_I$ thru $wt2_I$ coefficients obviously given as:

$$wu1_I = wv2_I = 1,\ wv1_I = wt1_I = wu2_I = wt2_I = 0. \tag{19a,b}$$

From equations (18a,b) and (4a,b) it is easy to verify that:

$$wu1_i = r1_i\, wu1_{i+1} + s1_i\, wu2_{i+1} + u1_i, \tag{20a}$$

$$wv1_i = r1_i\, wv1_{i+1} + s1_i\, wv2_{i+1} + v1_i, \tag{21a}$$

$$wt1_i = r1_i\, wt1_{i+1} + s1_i\, wt2_{i+1} + t1_i, \tag{22a}$$

$$wu2_i = r2_i\, wu1_{i+1} + s2_i\, wu2_{i+1} + u2_i, \tag{20b}$$

$$wv2_i = r2_i\, wv1_{i+1} + s2_i\, wv^{2}_{i+1} + v2_i, \tag{21b}$$

$$wt2_i = r2_i\, wt1_{i+1} + s2_i\, wt2_{i+1} + t2_i. \tag{22b}$$

Equations (20a-22b) together with "boundary conditions" (19a,b) allow the evaluations of the $wu1_i$ thru $wt2_i$ coefficients ($i = I-1, I-2,\ldots,1$). These will finally provide the solution vectors f_i, k_i, if F_I and k_I can be somehow determined. This is easily accomplished by eliminating the F_1, k_1, F_{I-1}, k_{I-1} unknowns in equations (3a,b) by means of the appropriate recursion formulas (18a,b) and by solving the resulting system of 2 equations in 2 unknowns, k_I, F_I by means of the Kramer's rule.

Fortran Implementation

The listing of a Fortran subroutine implementing the present algorithm is attached for convenience. Note that the possibility of using the same arrays for the recusion coefficients $u1_i$, $wu1_i$ . . . . , $t2_i$, $wt2_i$, has been exploited.

```
      SUBROUTINE PERINV(JEND)
C*********************************************************************
C* THE FOLLOWING SUBROUTINE INVERTS A COUPLED SET OF TWO            **
C* TRIDIAGONAL EQUATIONS WITH PERIODIC BOUNDARY CONDITIONS.         **
C* THE COEFFICIENTS OF THE DIFFERENCE EQUATIONS ARE A1 THRU         **
C* H1 AND A2 THRU H2. THE SOLUTION VECTORS ARE RETURNED TO          **
C* THE MAIN PROGRAM BY MEANS OF THE VECTORS H1 AND H2.          ******
C*********************************************************************
      COMMON A1(80),B1(80),C1(80),D1(80),E1(80),F1(80),H1(80),
     1A2(80),B2(80),C2(80),D2(80),E2(80),F2(80),H2(80)
      DIMENSION R1(80),S1(80),T1(80),U1(80),V1(80),
     1R2(80),S2(80),T2(80),U2(80),V2(80)
      JM1=JEND-1
      DENOM=1./(B1(1)*E2(1)-B2(1)*E1(1))
      R1(1)=DENOM*(E1(1)*C2(1)-E2(1)*C1(1))
      S1(1)=DENOM*(E1(1)*F2(1)-E2(1)*F1(1))
      T1(1)=DENOM*(E2(1)*H1(1)-E1(1)*H2(1))
      U1(1)=DENOM*(E1(1)*A2(1)-E2(1)*A1(1))
      V1(1)=DENOM*(E1(1)*D2(1)-E2(1)*D1(1))
      R2(1)=DENOM*(B2(1)*C1(1)-B1(1)*C2(1))
      S2(1)=DENOM*(B2(1)*F1(1)-B1(1)*F2(1))
      T2(1)=DENOM*(B1(1)*H2(1)-B2(1)*H1(1))
      U2(1)=DENOM*(B2(1)*A1(1)-B1(1)*A2(1))
      V2(1)=DENOM*(B2(1)*D1(1)-B1(1)*D2(1))
      DO 6 J=2,JM1
      B1N=A1(J)*R1(J-1)+D1(J)*R2(J-1)+B1(J)
      C1N=C1(J)
      E1N=A1(J)*S1(J-1)+D1(J)*S2(J-1)+E1(J)
      F1N=F1(J)
      AM1N=A1(J)*U1(J-1)+D1(J)*U2(J-1)
      AN1N=A1(J)*V1(J-1)+D1(J)*V2(J-1)
      H1N=H1(J)-A1(J)*T1(J-1)-D1(J)*T2(J-1)
      B2N=A2(J)*R1(J-1)+D2(J)*R2(J-1)+B2(J)
      C2N=C2(J)
      E2N=A2(J)*S1(J-1)+D2(J)*S2(J-1)+E2(J)
      F2N=F2(J)
      AM2N=A2(J)*U1(J-1)+D2(J)*U2(J-1)
      AN2N=A2(J)*V1(J-1)+D2(J)*V2(J-1)
      H2N=H2(J)-A2(J)*T1(J-1)-D2(J)*T2(J-1)
      DEN=1./(B1N*E2N-B2N*E1N)
      R1(J)=DEN*(E1N*C2N-E2N*C1N)
      S1(J)=DEN*(E1N*F2N-E2N*F1N)
      T1(J)=DEN*(E2N*H1N-E1N*H2N)
      U1(J)=DEN*(E1N*AM2N-E2N*AM1N)
      V1(J)=DEN*(E1N*AN2N-E2N*AN1N)
      R2(J)=-DEN*(B1N*C2N-B2N*C1N)
      S2(J)=-DEN*(B1N*F2N-B2N*F1N)
      T2(J)=-DEN*(B2N*H1N-B1N*H2N)
      U2(J)=-DEN*(B1N*AM2N-B2N*AM1N)
      V2(J)=-DEN*(B1N*AN2N-B2N*AN1N)
    6 CONTINUE
      U1(JEND)=1.
      V1(JEND)=0.
      T1(JEND)=0.
      U2(JEND)=0.
      V2(JEND)=1.
      T2(JEND)=0.
      DO 7 J=1,JM1
      K=JEND-J
      U1(K)=U1(K)+R1(K)*U1(K+1)+S1(K)*U2(K+1)
      V1(K)=V1(K)+R1(K)*V1(K+1)+S1(K)*V2(K+1)
      T1(K)=T1(K)+R1(K)*T1(K+1)+S1(K)*T2(K+1)
      U2(K)=U2(K)+R2(K)*U1(K+1)+S2(K)*U2(K+1)
      V2(K)=V2(K)+R2(K)*V1(K+1)+S2(K)*V2(K+1)
      T2(K)=T2(K)+R2(K)*T1(K+1)+S2(K)*T2(K+1)
    7 CONTINUE
      N=JEND
      M=JM1
      ALF1=A1(N)*U1(M)+B1(N)+C1(N)*U1(1)+D1(N)*U2(M)+F1(N)*U2(1)
      BET1=A1(N)*V1(M)+E1(N)+C1(N)*V1(1)+D1(N)*V2(M)+F1(N)*V2(1)
      GAMA1=H1(N)-A1(N)*T1(M)-C1(N)*T1(1)-D1(N)*T2(M)-F1(N)*T2(1)
      ALF2=A2(N)*U1(M)+B2(N)+C2(N)*U1(1)+D2(N)*U2(M)+F2(N)*U2(1)
      BET2=A2(N)*V1(M)+E2(N)+C2(N)*V1(1)+D2(N)*V2(M)+F2(N)*V2(1)
      GAMA2=H2(N)-A2(N)*T1(M)-C2(N)*T1(1)-D2(N)*T2(M)-F2(N)*T2(1)
      DEN=1./(ALF1*BET2-ALF2*BET1)
      H1(JEND)=DEN*(GAMA1*BET2-GAMA2*BET1)
      H2(JEND)=DEN*(GAMA2*ALF1-GAMA1*ALF2)
      DO 8 J=1,JM1
      H1(J)=U1(J)*H1(JEND)+V1(J)*H2(JEND)+T1(J)
      H2(J)=U2(J)*H1(JEND)+V2(J)*H2(JEND)+T2(J)
    8 CONTINUE
      RETURN
      END
```

Numerical Application

The present algorithm has been applied to a Spline 4[20] numerical solution of the following ordinary differential equation:

$$F''(x) + F(x) = (1 - 4\pi^2) \sin 2\pi x \ , \tag{23}$$

whose exact solution, $F(x) = \sin 2\pi x$, is available for comparison. The Spline 4 procedure[20], applied to the numerical integration of equation (23) in the range $0 \leq x < 1$ leads to a system of two coupled tridiagonal equations (1a-3b) with the following values of the coefficients:

$$\begin{aligned} &a1_i = c1_i = 1/12;\ b1_i = 5/6;\ d1_i = f1_i = 0;\ e1_i = 1; \\ &\qquad h1_i = (1 - 4\pi^2) \sin 2\pi(i - 1)h; \end{aligned} \tag{24a-e}$$

$$a2_i = c2_i = h^2/6;\ b2_i = 2h^2/3;\ d2_i = f2_i = -1;\ e2_i = 2;\ h2_i = 0. \tag{25a-e}$$

F_i and k_i are the functional and second derivative Spline 4[20] values at the nodal point $x_i [x_i = (i-1)h]$ and h is the step size ($h=1/I$).

Numerical solutions have been obtained for four values of I and the corresponding average truncation errors $\varepsilon(\varepsilon = \sum_{i=1}^{I} | F_i - \sin 2\pi(i-1)h|)/I)$, are given in Table I. The errors are proportional to h^4, as they should be, thus verifying the validity of the proposed algorithm. The solution corresponding to I = 160 required only 114 ms of CDC Cyber 175 computer.

N	20	40	80	160
ε	$.17 \cdot 10^{-4}$	$.11 \cdot 10^{-5}$	$.69 \cdot 10^{-7}$	$.43 \cdot 10^{-8}$

TABLE I

☆U.S.Government Printing Office: 1980 — 657-084/768